CHEMICAL ENGINEERING TRANSACTIONS
VOL. 42, 2014
A publication of AIDIC
The Italian Association of Chemical Engineering
www.aidic.it/cet
Guest Editors: Petar Sabev Varbanov, Neven Duić

ISBN 978-88-95608-33-4; **ISSN** 2283-9216
DOI:10.3303/CET1442004

Assessment of Inlets Capacity for Inundation Diminution in Urban Watershed

In-Hyeok Park, Jeong-Yong Lee, Seung-Chul Lee, Sung-Ryong Ha*

[a]Department of Urban Engineering, Chungbuk National University, Republic of Korea
simplet@chungbuk.ac.kr

Inundation has been highlighted as a major disaster in urban areas due to the emergence of climate change effects on urban hydrology including the deficit of sewer capacity and reduction of delivery and retention times. Furthermore, inundation simulation has been made possible in urban areas because of high resolution topographic data being made available through LiDAR surveys which have provided accurate information on surface conditions. However, recent research on urban inundation has been focused on terrain resolution or building treatment. Although inlets by roads play an important role for draining surface flow, spatial distribution of inlets tends to be neglected in inundation simulations. It is difficult to construct pervious areas in already developed places such as urban areas for disaster management, the spatial distribution of inlets should be considered for the sustainable development of urban areas to avoid inundation disasters. This study aims to investigate the effect of spatial distribution of culverts on urban inundation using Cartesian based terrain as topographical data for a dual-drainage model, and to figure out the proper distribution of culverts combined with pervious distribution areas for a reduction of inundation.

1. Introduction

Urban inundation is more frequently occurring now than in the past, this is a result of not only an increase of torrential storms due to climate change but also due to runoff interference caused by surface facilities, such as buildings, connected with a deficit of discharge capacity of sewer pipes. To establish countermeasures against urban inundation, it is required to elaborately simulate surface runoff considering infrastructures as well as interaction between the hydraulic head of surface runoff and the discharge capacity of conduits. According to the guidelines for inlets installation which play an important role in reducing urban inundation, the gaps between inlets are generally allocated between 10~30 cm taking into consideration road width and terrain slope, and the gaps should be shortened in the case of a repeatedly inundated zone (Ken et al., 2011). The occurrence and possible effects of surface flooding depend much more on local constraints and surface characteristics, which are much more difficult described physically, and these data are usually not available in practice (Schmitt et al., 2004). However, the opening size of inlets is not seen as important as the placement of inlets. Especially, most of simulation modelling has a tendency to neglect of inlets distribution because it is difficult to count for the distribution and fluid mechanics of inlets. This study aims to investigate the optimal opening size of inlets for minimizing inundation and to assess diminution effects in accordance with the opening size of inlets. The simulation of inundation considered inundation depth/velocity, runoff velocity, flow depth/velocity of conduits, and re-entering surface runoff into conduits using a 2D inundation model.
Conventionally it was considered that the deficient carrying capacity of the sewer system was the main cause of flooding in urbanized districts. As the size of impervious area grew, basin related parameters showed a decrease in the delivery time and an increase in the runoff velocity. These two water components caused an unbalanced water head. To elucidate the spatial causes of the flooding, the concept of contribution rate was adopted with the consideration of dynamic linkage of drainage networks and spatial distribution of manholes beneath those lines.

Please cite this article as: Park I.H., Lee J.Y., Lee S.C., Ha S.R., 2014, Assessment of inlets capacity for inundation diminution in urban watershed, Chemical Engineering Transactions, 42, 19-24 DOI:10.3303/CET1442004

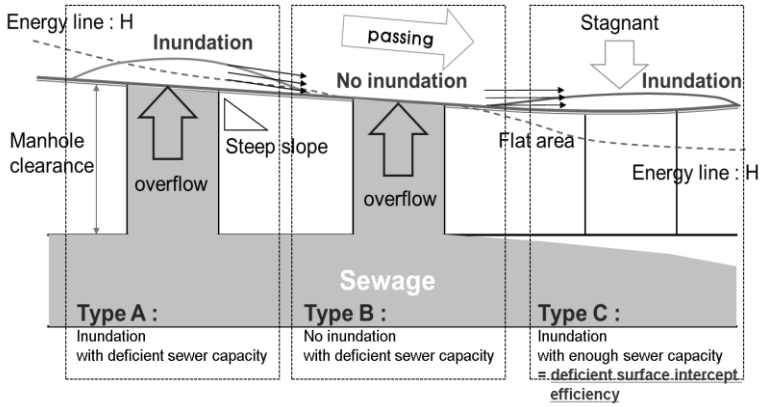

Figure 1: Classification of three types of inundation considering hydraulic conditions

In contrast with the conventional scheme of inundation (Djordjevic et al., 1999), this study classified three types of urban inundation considering hydraulic head (Figure 1). Type A is similar with the conventional inundation scheme, which is flooding under deficient discharge capacity of sewers. Type B is the absence of flooding under the deficient discharge capacity and type C is flooding under sufficient discharge capacity. From the urban watershed, overflowing surface water runs through the basin according to the terrain slope and the overland water component which was gathered in a lower terrain zone this was causing the overflowing effects in Type A and Type C. To be more specific, the velocity of the surface flow in the flooded zone has increased to the level of surpassing the limit of critical velocity causing hindering effects of surface flow entering the manhole.

2. Materials and methods

2.1 Inlets capacity

Inlets are the major components of urban drainage systems which drain surface flow into sewer pipes. To calculate design capacity of the inlets, some usually require a momentary peak flow rate while others require runoff hydrographs that provide an estimation of runoff volumes. In the case of inundation by an extreme event exceeding the design storm, the function of the inlets were decreased, thus surface water stagnated because the inlets were working abnormally. However, there were no considerations of inlet effects, which meant that surface flow drained into the sewer system without loss in the previous research. In this study, inlet capacity is adopted as a non-dimensional constant, which means the currently installed maximum allowable area of the inlets to drain surface flow into the sewer system for preventing urban areas from inundation or flooding. The inlet capacity is described in the Eq (1).

$$\rho = \left(\sum_{i=1}^{n} \alpha_i \right) 10^4 / A \quad (1)$$

where ρ = inlet capacity as a non-dimensional parameter, α_i = the hydraulic area (opening area) of i inlet (m^2), and A = the watershed area (ha).

The kind of inlets was classified with three types; curb inlets, grating inlets and combination inlets. Because most of inlets which were installed in the study area were grating inlets, we adopted fluid mechanics of grating inlets (Guo et al., 2007). The capacity of grate inlets in sumps is given by the following Eq (2).

$$Q_o = N_o C_o \sqrt{2g} W_g L_g d^{\frac{1}{2}} \quad (2)$$

where Q_o= orifice flow, W_g= grate width, N_o= orifice area opening ratio, C_o = orifice discharge coefficient, L_g= grate length, and d= water depth.

2.2 Study area

The study area is a frequently flooded zone in the city of Cheongju, Korea. It is located on the right side of the Moosim River, which crosses through Cheongju. Wooam Mountain (EL.343 m) is situated in the northeast area and the Moosim River flows southwest. Figure 2 shows the study area which is a typical residential area, mostly composed of detached housing and the centre district of the site is closely compacted with commercial facilities. The ratio of the impervious area of the site is 96 % and the total basin area is 11.84 km^2. The number of inlets was found to be 1,013 EA, and the average hydraulic area

of the inlets was about 0.6 m^2. So the ρ of the study area was estimated at 0.43. The dashed lines indicated the sewer pipes and the dots meant inlets of study area.

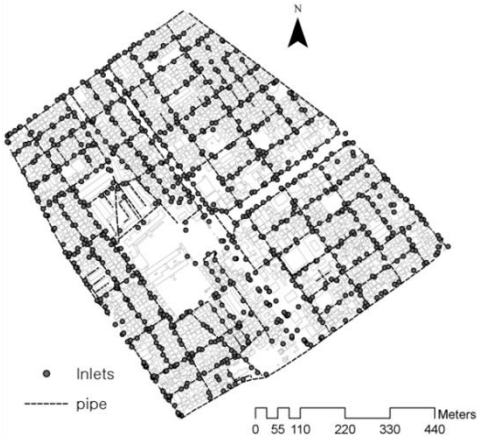

Figure 2: The study area and inlet distribution status

2.3 Model description

The concept of a dual-drainage system, proposed by Djordjevic et al. (1999) has been created to supplement the limited assumptions of the conventional urban flooding model including the limitations of modelling reproductive capacity, which contains the disappearing or detained surface water component in a manhole. In this study, an XP-SWMM 2-D model developed by Hydrosoft Inc. has been selected to simulate the inundation impact. XP-SWMM 2-D is a coupled modelling system which is composed of SWMM (Storm Water Management Model) developed by EPA and TUFLOW (WBM Oceanics, 2003), which is a fully dynamic engine used to analyse 2 dimensional flooding developed by Australia WBN Inc.

- Governing equation of subsurface flow [1-D unsteady gradually varied flow equation (Lai, 1986)]:

$$\frac{\partial A}{\partial t}+\frac{\partial Q}{\partial s}-q_1+q_2=0 \tag{3}$$

$$\frac{\partial Q}{\partial t}+\frac{\partial}{\partial s}\left(\frac{Q^2}{A}\right)-gA\left(S_0-\frac{\partial d}{\partial s}-S_f\right)+q_2\left(\frac{Q}{A}\right)=0 \tag{4}$$

where, A and Q are the cross-sectional area and discharge of the channel respectively, q_1 is the lateral inflow per unit length flowing from the floodplain to the channel, q_2 is the lateral outflow per unit length flowing from the channel to the floodplain, s is the coordinate along the longitudinal direction, g is the gravitational acceleration, S_0 is the bed slope, d is the flow depth, S_f is the friction slope - Governing equation of surface flow (inundation):

$$\frac{\partial C}{\partial t}+\frac{\partial(Hu)}{\partial x}+\frac{\partial(H\gamma)}{\partial y}=0 \tag{5}$$

$$\frac{\partial u}{\partial t}+u\frac{\partial u}{\partial x}+\gamma\frac{\partial u}{\partial y}-c_f\gamma+g\frac{\partial C}{\partial x}+gu\left(\frac{n^2}{H^{\frac{4}{3}}}+\frac{f_l}{2g\partial x}\right)\sqrt{u^2+\gamma^2}-\mu\left(\frac{\partial^2 u}{\partial x^2}+\frac{\partial^2 u}{\partial y^2}\right)+\frac{1}{\rho}\frac{\partial P}{\partial x}=F_x \tag{6}$$

$$\frac{\partial \gamma}{\partial t}+u\frac{\partial \gamma}{\partial x}+\gamma\frac{\partial \gamma}{\partial y}-c_f u+g\frac{\partial C}{\partial y}+g\gamma\left(\frac{n^2}{H^{\frac{4}{3}}}+\frac{f_l}{2g\partial y}\right)\sqrt{u^2+\gamma^2}-\mu\left(\frac{\partial^2 \gamma}{\partial x^2}+\frac{\partial^2 \gamma}{\partial y^2}\right)+\frac{1}{\rho}\frac{\partial P}{\partial y}=F_y \tag{7}$$

where, C is the water elevation, u is the mean velocity in the direction of the X-axis, γ is the mean velocity in the direction of the Y-axis, H is the depth, t is the time, x is the length in the direction of the X-axis, y is the length in the direction of the Y-axis, c_f is the Coriolis force coefficient, n is the Manning roughness of channel, f_l is the form loss coefficient, μ is the momentum horizontal dispersion coefficient, P is the atmospheric pressure, ρ is the density of water, F_x and F_y are each the total sum of external forces in the direction of the X-axis and the Y-axis respectively.

3. Results and discussions

3.1 Estimation of optimum inlet capacity

To calculate the optimum capacity for inlets in this study area, the test bed which was located in the centre of the study area consisting of the same inlets was extracted. In the test bed, there were 58 grate type inlets. The inlet capacity scenario was designed from 0.24 to 0.95 considering the average inlet capacity of

the study area, and the rainfall adopted here was varied from 60 mm/hr to 110 mm/hr of the designed storm. Inundation area and volume were analysed varying the inlets capacity and the designed storm at the peak occurrence of inundation.

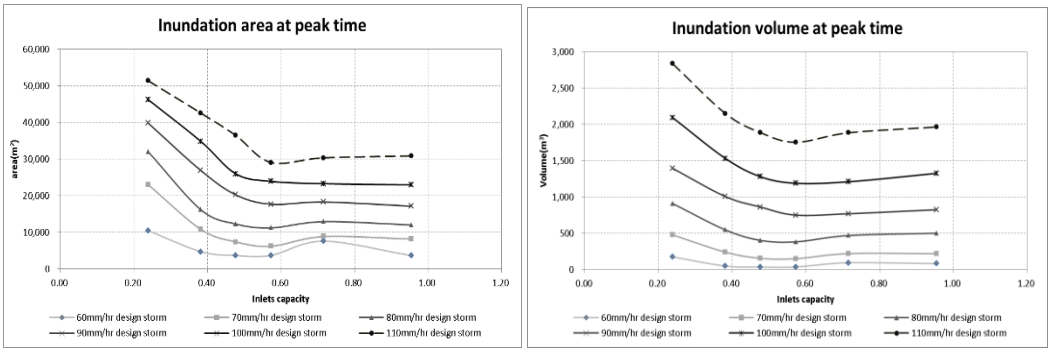

Figure 3: Variation of inundation volume and area according to inlet capacity changes at inundation peak

(a) 0.25 inlet capacity (b) 0.75 inlet capacity (c) 1.0 inlet capacity

Figure 4: Changes of inundation area by altering inlet capacity in the case of 110mm/hr at inundation peak

The inundation peak could be assumed when both the inundation area and volume were largest. Figure 3 shows the inundation area and the volume of the study area at the inundation peak according to inlet capacity changes in the case of 110 mm/h of the designed storm. The largest inundation area appeared at 0.25 of the inlets capacity as 5.1 ha while the smallest inundation area appeared at 0.75 and 1.0 of the inlets capacity as 3.0 ha among them (Figure 4). However, in the case of inundation volume, the 0.25 case revealed the biggest volume whereas the 0.7 case showed the smallest volume contrary to the inundation area. According to this figures, optimum inlet capacity to minimize the inundation area and volume was estimated as 0.57. If the inlet capacity is bigger than 0.6, the efficiency of intercepting surface water has a tendency to decline.

In the case of adapting the 0.25 inlet capacity, the inundation area and volume were calculate as large because the efficiency of intercepting surface water was drastically decreased by small inlet capacity due to step conditions. Otherwise, in the case of exceeding 0.6 inlet capacity adaptation, a bottleneck phenomenon in the conduits was the main reason for large inundation volume, which was caused by reaching maximum sewer carrying capacity earlier. So, 0.6 inlet capacity could be determined as the optimal capacity of inlets for this study area to minimize the inundation hazard. Although the current inlet capacity of this study area is about 0.4 as described above, the hydraulic area of the inlets was usually disturbed with garbage. This is the reason for the frequent inundation observed in this study area.

3.2 Comparison of inundation characteristics between current inlet capacity and optimal inlet capacity

To figure out the difference between current inlet capacity (0.4) and optimal inlet capacity (0.6), the inundation analysis was performed using an observed storm. A relatively lower inundation depth, with less than 20 cm, was represented in the western region of the site with low elevation. The average, minimum and maximum of inundated depth shows 21.2 cm, 3.5 cm and 76.1 cm respectably in the case of 0.4 inlet capacity. For the 0.6 inlet capacity adaptation, average, minimum and maximum of inundated depth shows 20.1 cm, 3.45 m and 74.8 cm respectably. To analyse the spatial inundation dispersion and sewer carrying capacity status, a distribution map of the spare space of each manhole at 17:45 has been depicted in Figure 5. When considering the structural characteristics of tree-type pipe networks flowing into the intercepting sewer line, the movement of hydrological components had an irregular pattern compared to the movement of a block system.

Therefore, inundation on the major inundation zones has been caused by surface runoff including sewer overflows from a branch sewer line of the site, which are naturally flowing down to the lower elevation due to gravity. These propagated inundation effects on the surface runoff caused by overflows of the branch sewer can be examined by the existence of spare capacity at a manhole in the major inundation zone. From the modelling result, spare space of manholes in the major inundation zones has reached approximately 40 cm or 45 cm except for some of the sites. Inundation of the Major inundation zones has been caused by a hindering effect of inflows into the manholes not by the deficient carrying capacity of the sewer system in the flooded zone (Park et. al., 2014).

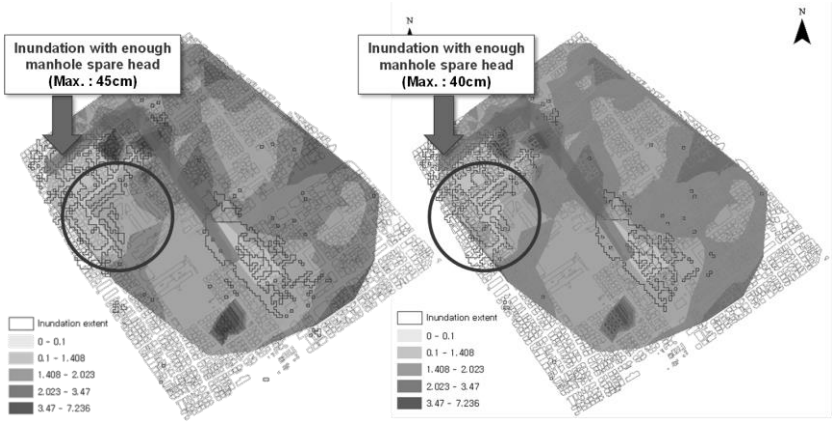

(a) 0.4 inlets capacity *(b) 0.6 inlets capacity*

Figure 5: Distribution map of spare space for the manholes by inlet capacity changes

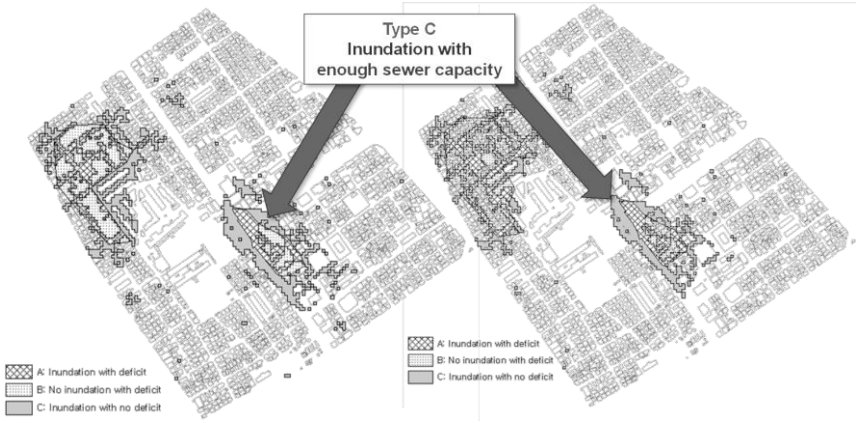

(a) 0.4 inlets capacity *(b) 0.6 inlets capacity*

Figure 6: Classification of inundation types according to inlets capacity adaptation

3.3 Changes of inundation types according to inlet capacity variation

Figure 6 shows the classification results; Type A is flooding under the deficient carrying capacity of the sewer, Type B is no flooding under the deficient carrying capacity and a Type C is flooding under sufficient carrying capacity. In the case the 0.4 inlet capacity, each flooded area shows 24 % for Type A (1.8 ha), 31 % for Type B (2.3 ha) and 45 % for Type C (3.4 ha). Otherwise, each flooded area shows 31 % for Type A (2.2 ha), 31 % for Type B (2.5 ha) and 45 % for Type C (2.3 ha) in the 0.6 inlet capacity. Overflowing surface water runs through the basin according to the terrain slope and the overland water component which was gathering in the lower terrain zone was causing the overflowing effects in the Type A and Type C region.

Figure 7 shows the frequency of overflow volume from the manholes and its cumulative percentage. From these figures, the frequency of overflow volume is linearly increased by overflow incrementally except in the case 10 m^3 of overflow volume in the case of 0.4 inlet capacity. However, in the case of 0.6 inlet capacities, the overflowing pattern of the 0.4 inlets disappeared and the percentage for less than 200 m^3 of overflow volume is 5 % lower than the 0.4 inlet capacity adaptation at 89.1 %. It is relatively easy to find regions needing a high priority rehabilitation of the sewer system to the 0.6 inlet capacity, while deficient

carrying capacity with not enough hydraulic area to drain surface water make the hazard of inundation difficult to solve. One thing that we need to focus on is trunk sewers with 0.4 inlet capacity, only one site overflowed. However, with the sufficient carrying capacity of the sewer line, overflows were observed in the major inundation zone. It was caused by surpassing the critical level of velocity in the inlet inflows due to the water head of surface flow from the upper basin district.

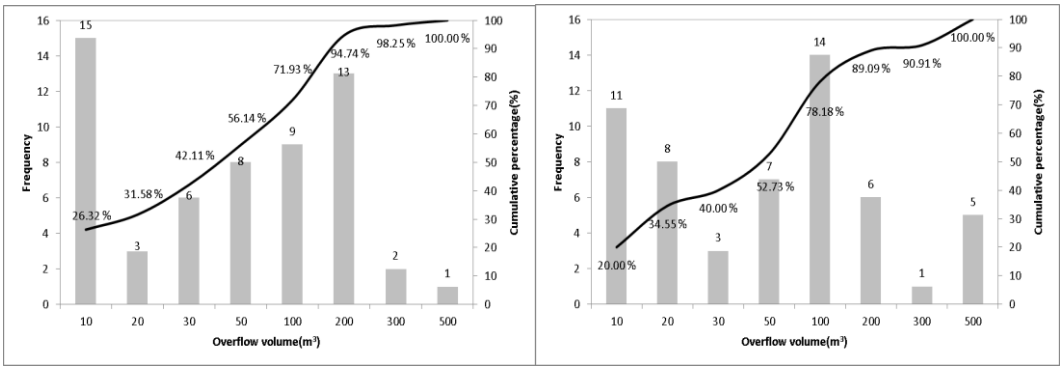

(a) 0.4 inlets capacity *(b) 0.6 inlets capacity*

Figure 7: Frequency and cumulative percentage of overflow volume by inlets capacity changes

4. Conclusions

In this study, the optimal opening size of inlets for minimizing inundation was investigated and the diminution effects in accordance with opening size of inlets was assessed using inundation depth and area. The simulation of inundation considered inundation depth/velocity, runoff velocity, flow depth/velocity of conduits, and re-entering surface runoff into conduits using a 2D inundation model.

With the dual drainage system model, characteristics of inundation have been analysed with the condition of a fifty times a year frequency of rainfall (total rainfall 165 mm) on the repeatedly flooded zone in the City of Cheongju. The carrying capacity of the sewer system has been assessed with the consideration of inlets capacity. In the case of the main sewer system, even though the sewer line has enough carrying capacity, surface runoff originated from the upper basin formulated the head of surface flow and inundation sustained because of not enough inlet capacity. For the case of branch sewer lines, when an optimal inlet capacity was adopted the inundation area and volume were reduced whereas the inundation from main sewer lines was increased.

For a more exact evaluation of inundation influence rage to minimize hazard, propagation effects of inundation through more precise modelling and deliberate analysis of the results needs to be done with 2-D simulation of surface flow considering inlets capacity.

Acknowledgement

This research was supported by the National Research Foundation of Korea (NRF) under the Korean government (Ministry of Education and Science Technology (MEST)) in 2012 [No.2011-0028914].

References

Bales J.D., Wagner C.R., 2009. Sources of uncertainty in flood inundation maps, Journal of Flood Risk Management, 2, 139-147.

Djordjevic S., Prodanovic D., Makximovic C., 1999. An Approach to Simulation of Dual Drainage, Water Science and Technology 39, 5, 95-103.

Guo James C.Y., Mackenzie Ken A., Mommandi A., 2007. Design of Street Sump inlet, Journal of Hydraulic Engineering 135, 11, 1000-1004.

Lai C.T., 1986. Numerical Modelling on Unsteady Open-Channel Flow, In Advances in Hydroscience, edited by Yen, B.C., 189-250, Academic Press, New York, USA.

Park I.-H., Lee J.-Y., Lee J.-H., Kim B.-S., Ha S.-R., 2014, Evaluation of the Causes of Inundation in a Repeatedly Flooded zone in the City of Cheongju, Korea using a 1D/2D Model, Water Science and Technology, 69(11), 2175-2183, doi: 10.2166/wst.2014.077.

Schmitt Theo G., Thomas M., Ettrich N., 2004. Analysis and Modeling of Flooding in Urban drainage systems, Journal of Hydrology, 299, 300-311.

WBM Oceanics (2003) “TUFLOW (and ESTRY) User Manual - GIS Based 2D/1D Hydrodynamic Modelling”, User Manual, Brisbane, Australia.